Primate immunodeficiency virus Vpx and Vpr counteract transcriptional repression of proviruses by the HUSH complex

Leonid Yurkovetskiy[1], Mehmet Hakan Guney[1], Kyusik Kim[1], Shih Lin Goh[1], Sean McCauley[1], Ann Dauphin[1], William Diehl[1], and Jeremy Luban[1,2]*

[1]Program in Molecular Medicine, University of Massachusetts Medical School, Worcester, MA 01605, USA

[2]Department of Biochemistry and Molecular Pharmacology, University of Massachusetts Medical School, Worcester, MA 01605, USA

*Correspondence: jeremy.luban@umassmed.edu (J.L.)

1   Drugs that inhibit HIV-1 replication and prevent progression to AIDS do not

2   eliminate HIV-1 proviruses from the chromosomes of long-lived CD4$^+$ memory T

3   cells. To escape eradication by these antiviral drugs, or by the host immune

4   system, HIV-1 exploits poorly defined host factors that silence provirus

5   transcription. These same factors, though, must be overcome by all retroviruses,

6   including HIV-1 and other primate immunodeficiency viruses, in order to activate

7   provirus transcription and produce new virus. Here we show that Vpx and Vpr,

8   proteins from a wide range of primate immunodeficiency viruses, activate

9   provirus transcription in human CD4$^+$ T cells. Provirus activation required the

10 DCAF1 adaptor that links Vpx and Vpr to the CUL4A/B ubiquitin ligase complex,

11 but did not require degradation of SAMHD1, a well-characterized target of Vpx

12 and Vpr. A loss-of-function screen for transcription silencing factors that mimic

13 the effect of Vpx on provirus silencing identified all components of the Human

14 Silencing Hub (HUSH) complex, FAM208A (TASOR/RAP140), MPHOSPH8 (MPP8),

15 PPHLN1 (PERIPHILIN), and MORC2. Vpx associated with the HUSH complex

16 components and decreased steady-state levels of these proteins in a DCAF-

17 dependent manner. Finally, *vpx* and FAM208A knockdown accelerated HIV-1 and

18 SIV$_{MAC}$ replication kinetics in CD4$^+$ T cells to a similar extent, and HIV-2 replication

19 required either *vpx* or FAM208A disruption. These results demonstrate that the

20 HUSH complex restricts transcription of primate immunodeficiency viruses and

21 thereby contributes to provirus latency. To counteract this restriction and

22 activate provirus expression, primate immunodeficiency viruses encode Vpx and

23 Vpr proteins that degrade HUSH complex components.

1

24   When provided *in trans*, many primate immunodeficiency virus Vpx and Vpr orthologues

25   increase HIV-1 reverse transcription and transduction efficiency in dendritic cells,

26   macrophages, and resting CD4$^+$ T cells (Baldauf et al., 2012; Goujon et al., 2006; Lim et

27   al., 2012; Sharova et al., 2008; Srivastava et al., 2008). As substrate adaptor proteins

28   for the DCAF1-CUL4A/B E3 ubiquitin ligase, Vpx and Vpr increase the concentration of

29   deoxynucleotide triphosphate (dNTP) levels in target cells by degrading the

30   deoxynucleotidetriphosphate (dNTP) hydrolase SAMHD1 (Hrecka et al., 2011; Laguette

31   et al., 2011; Lim et al., 2012). Nonetheless, Vpx and Vpr have additional effects on

32   expression of transduced reporter genes that are not explained by SAMHD1

33   degradation or by increase in dNTP concentration (Goh et al., 1998; Miller et al., 2017;

34   Pertel et al., 2011a; Reinhard et al., 2014).

35   To better understand the effect on provirus reporter gene expression, *vpx* was

36   introduced before, during, or after transduction of a reporter gene (Fig. 1a). Jurkat CD4$^+$

37   T cells were transduced with a dual-promoter, lentiviral vector that expresses codon-

38   optimized SIV$_{MAC}$251 *vpx* from the spleen focus forming virus (SFFV) promoter and

39   puromycin acetyltransferase (puro^R) from the PPIA (CypA) promoter (Neagu et al.,

40   2009; Reinhard et al., 2014) (Lenti 1 in the Fig. 1a time-line, Supplementary Fig. 1a, and

41   Supplementary Table 1). A control Lenti 1 vector was used that lacks *vpx*

42   (Supplementary Fig. 1a). Puromycin was added to the culture on day three to select

43   those cells that had been transduced with Lenti 1. On day seven, cells were transduced

44   with a second lentivector bearing a codon-optimized *gag-gfp* reporter gene expressed

45   from the SFFV promoter, as well as SIV$_{MAC}$251 *vpx* expressed from the CypA promoter

46   (Lenti 2 in the Fig. 1a timeline and Supplementary Fig.1a). A control Lenti 2 vector was

2

47   used that lacks *vpx* (Supplementary Fig.1a). On day ten, virus-like particles (VLPs)

48   containing Vpx protein were added to the twice-transduced cells (Fig. 1a). As controls,

49   VLPs lacking Vpx were used, or no VLPs were added. On day fourteen, the percent

50   GFP$^+$ cells under each condition was assessed by flow cytometry using standard gating

51   for viable, singlet, lymphoid cells (Supplementary Figure 1b). Vpx increased the

52   percentage of GFP$^+$ cells, whether *vpx* was transduced before, or concurrent with,

53   reporter gene transduction, or if Vpx protein was delivered by VLPs after reporter gene

54   transduction (Fig. 1b and Supplementary Fig 1c; n=3 biological replicates, $p<0.02$, 1-

55   way ANOVA with Dunnett post-test). These results suggest that the transduced reporter

56   gene was actively silenced and that *vpx* overcame reporter silencing.

57   To confirm that the findings in Fig. 1b were due to effects of *vpx* on

58   transcriptional silencing of the reporter gene, and not due to effects on transduction

59   efficiency, Jurkat T cells were first transduced with a vector in which the *gag-gfp*

60   reporter gene was expressed from the SFFV promoter and blasticidin-S deaminase

61   (blasti^R) was expressed from the CypA promoter. Four days after transduction with the

62   reporter vector and selection with blasticidin, cells were either challenged with Vpx$^+$

63   VLPs, or transduced and selected with the dual-promoter lentivector encoding *vpx* and

64   *puroR* (Lenti 1 in Supplementary Fig. 1a). Four days later the GFP signal was at

65   background levels unless Vpx was provided, either by VLPs (Fig. 1c) or by *vpx*

66   transduction (Fig. 1d). The effect of *vpx* on reporter gene expression was confirmed by

67   qRT-PCR for the reporter mRNA (Supplementary Fig. 1d). Reporter gene silencing and

68   reactivation by Vpx was not specific to the SFFV promoter since GFP signal was similar

69   when the reporter gene was expressed from the human EEF1A1 (EF1α) promoter or

3

70 from the Herpes simplex virus type 1 thymidine kinase (TK) promoter (Supplementary

71 Fig. 1e). These results demonstrate that Vpx overcomes transcriptional silencing of the

72 provirus.

73   To determine if the ability to activate transcription of silenced proviruses is

74 peculiar to $SIV_{MAC}251$ Vpx, representative Vpx and Vpr orthologues, selected from

75 across the phylogeny of primate immunodeficiency viruses, were examined. All Vpx

76 proteins tested, $SIV_{DRL}D3$, $SIV_{RCM}NG411$, $SIV_{AGI}00CM312$, $SIV_{RCM}02CM8081$,

77 $SIV_{MND2}5440$, HIV-2$_{ROD}$, $SIV_{MAC}251$, and $SIV_{MNE}027$, had transactivating activity in

78 human cells (Fig. 1e and Supplementary Fig 1f). Conservation of this activity in human

79 cells among such divergent SIV orthologues was surprising given that $SIV_{RCM}NG411$

80 Vpx and $SIV_{MND2}5440$ Vpx do not degrade human SAMHD1, but they do degrade the

81 SAMHD1 orthologue from their cognate primate host species (Lim et al., 2012). Several

82 Vprs from SIVs that lack Vpx, including $SIV_{MUS2}CM1246$, $SIV_{AGM}Ver9063$, $SIV_{AGM}TAN1$,

83 $SIV_{MND1}GB1$, and $SIV_{LST}524$, also activated transcription of silent proviral reporters in

84 human cells (Fig. 1e and Supplementary Fig. 1f). Results could not be obtained from

85 this experimental system concerning the activity of Vprs encoded by $SIV_{CPZ}TAN3$, HIV-

86 1$_{U14788}$ (Group P), $SIV_{GOR}CP684con$, HIV-1$_{MVP5180}$ (Group O), HIV-1$_{NL4-3}$ (Group M),

87 $SIV_{CPZ}LB7$, and $SIV_{RCM}02CM8081$, presumably because these orthologues caused cell

88 cycle arrest and toxicity (Chang et al., 2004; Goh et al., 1998; He et al., 1995; Re et al.,

89 1995) (indicated by $\varnothing$ in Fig. 1e). Vpx and Vpr sequence variability is among the highest

90 observed for lentiviral coding sequences (McCarthy and Johnson, 2014); the sequences

91 shown in Fig. 1e have an average amino acid identity of only 27%. Such diversity likely

92 reflects rapidly evolving, host-pathogen interfaces (Fregoso et al., 2013), and precluded

93   activity predictions based on amino acid sequence conservation to guide the

94   engineering of loss-of-function mutations.

95   To gain insight into the mechanism by which Vpx overcomes transcriptional

96   silencing of lentiviral transgenes, a loss-of-function screen was performed focusing on

97   genes reported to contribute to silencing of retroviruses and other transcriptional targets

98   (Chéné et al., 2007; Peterlin et al., 2017; Tchasovnikarova et al., 2015, 2017; Wang and

99   Goff, 2017; Weinberg and Morris, 2016; Wolf and Goff, 2007). Jurkat T cells were

100   transduced with lentivectors that confer puromycin resistance and express shRNAs

101   (Pertel et al., 2011b) targeting either AGO1, AGO2, AGO3, DNMT3A, HDAC1, HP1,

102   SUV39H1, SUV39H2, PIWIL2, TRIM28, SETDB1, FAM208A, MPHOSPH8, PPHLN1, or

103   MORC2. After selection for five days with puromycin, cells were transduced with the

104   Lenti 2 *gag-gfp* reporter vector without *vpx* (Supplementary Fig. 1a). Four days later, the

105   change in expression of the *gfp* reporter due to the knockdowns was calculated as a

106   percentage of the activity observed in a separate population of Jurkat cells transduced

107   to express *vpx* (Fig. 2a). A given gene was implicated as a transcriptional silencing

108   factor for the provirus reporter gene if the three shRNA targets for that gene differed

109   significantly from that of the luciferase knockdown control ($p<0.05$, 1-way ANOVA with

110   Dunnett post-test). shRNAs targeting each of the three core components of the Human

111   Silencing Hub (HUSH) complex, FAM208A, MPHOSPH8, and PPHLN1, increased

112   reporter gene expression (Fig. 2a).

113   The effect on reporter gene expression in Jurkat T cells of the most effective

114   shRNA target sequences for FAM208A, MPHOSPH8, and PPHLN1 is shown in Fig. 2b.

115   The effectiveness of the knockdown of each of the HUSH complex components in

5

116   Jurkat cells was confirmed by immunoblotting lysate from these cells with antibodies

117   specific for FAM208A, PPHLN1, or MPHOSPH8 (Fig. 2c). As previously reported

118   (Tchasovnikarova et al., 2015), knockdown of any individual HUSH complex component

119   caused a decrease in the level of each of the other components. Similar results on

120   reporter gene expression were obtained when FAM208A, MPHOSPH8, or PPHLN1

121   were knocked down in primary human CD4$^+$ T cells (Fig. 2d). Knockdown of each of the

122   HUSH complex components, then, had the same effect as *vpx* on lentiviral reporter

123   gene expression (Fig. 2b and d and Supplementary Fig 2a). These results demonstrate

124   that the HUSH complex is critical for provirus silencing and raise the possibility that Vpx

125   acts as a substrate adaptor targeting HUSH components to DCAF1 and the CUL4A/B

126   E3 ubiquitin ligase complex for degradation, in the same way that Vpx targets SAMHD1

127   (Hrecka et al., 2011; Laguette et al., 2011).

128   To determine if Vpx promotes the degradation of HUSH complex components,

129   lysate from cells transduced to express $SIV_{MAC}251$, $SIV_{MND2}5440$, or $SIV_{RCM}NG411$ *vpx*

130   was immunoblotted with antibodies specific for FAM208A, PPHLN1, or MPHOSPH8. All

131   three Vpx proteins reduced the steady-state level of all three core HUSH complex

132   components (Fig. 2e). Among the three HUSH components, though, FAM208A protein

133   levels were decreased more than the other two components (Fig. 2f) so ongoing

134   experiments focused on the effect of Vpx on FAM208A. Indeed, in addition to the three

135   Vpx proteins assessed in Fig. 2e, the other Vpx and Vpr orthologues shown to have

136   transactivation activity in Fig 1e and Supplementary Fig 1f (HIV-2$_{ROD}$ Vpx, $SIV_{MNE}027$

137   Vpx, $SIV_{DRL}D3$ Vpx, $SIV_{AGM}TAN1$ Vpr, $SIV_{MND1}GB1$ Vpr, and $SIV_{LST}524$ Vpr) all

138   decreased the levels of FAM208A (Supplementary Figs. 2b and c).

139   To assess whether disruption of FAM208A protein levels by Vpx was dependent

140   upon the DCAF1 adaptor for the CUL4A/B ubiquitin ligase complex, as is the case for

141   SAMHD1 (Sharova et al., 2008; Srivastava et al., 2008), Jurkat T cells were transduced

142   with a lentivector that knocks down DCAF1 (Pertel et al., 2011a), or with a control

143   knockdown vector. After selection with puromycin the cells were exposed for 18 hrs to

144   SIV VLPs bearing Vpx, control VLPs that lacked Vpx, or no VLPs. In the DCAF1

145   knockdown cells, FAM208A protein levels were unchanged by Vpx, indicating that

146   FAM208A disruption by Vpx was dependent upon DCAF1 (Fig. 2g).

147   Degradation of SAMHD1 requires direct interaction with Vpx or Vpr (Lim et al.,

148   2012). To determine if Vpx similarly associates with proteins of the HUSH complex, HA-

149   tagged FAM208A was co-transfected into HEK293 cells with FLAG-tagged $SIV_{MAC}251$

150   Vpx or $SIV_{RCM}02CM8081$ Vpx. When anti-FLAG antibody was used to

151   immunoprecipitate either of the two Vpx proteins from the soluble cell lysate, HA-

152   FAM208A was detected in the immunoprecipitate (Fig. 2h). The strength of the

153   FAM208A signal in the Vpx pull-out increased when the co-transfected HEK293 cells

154   were incubated with the proteasome inhibitor PR171, or when wild-type $SIV_{MAC}251$ Vpx

155   was replaced in the transfection by a mutant (Q76A) that is incapable of binding DCAF1

156   (Pertel et al., 2011a; Srivastava et al., 2008) (Fig. 2h and Supplementary Figs. 2d,e).

157   These results demonstrate that FAM208A associates with Vpx and that the interaction

158   results in proteasome-mediated degradation of FAM208A.

159   The experiments described above examined the effect of Vpx or Vpr on HIV-1

160   proviruses in which the reporter gene was transcribed by a heterologous promoter,

161   either human EF1α, HSV TK, or the SFFV LTR (Figs 1 and 2, and Supplementary Fig.

7

162   1). To determine if Vpx is capable of activating a reporter gene driven by the HIV-1 LTR,

163   the TNFα-responsive, J-Lat A1 clonal cell line was used (Jordan et al., 2003). In this

164   experimental model of provirus latency, the HIV-1 LTR drives expression of a bicistronic

165   mRNA encoding *tat* and *gfp* (Fig. 3a). Transduction with a lentivector expressing

166   SIV$_{mac}$251 Vpx, or knockdown of FAM208A, caused comparable increase in the percent

167   GFP$^+$ J-Lat A1 cells, whether the cells were stimulated with TNFα or not (Fig. 3b and c).

168   Transduction of the J-Lat A1 cell line with lentivectors expressing *vpx* encoded by

169   SIV$_{RCM}$02CM8081 or SIV$_{MND2}$5440, as well as with *vpr* encoded by SIV$_{MND1}$GB1 or

170   SIV$_{AGM}$TAN1, caused similar increase in expression of the LTR-driven reporter gene

171   (Supplementary Fig 3a).

172   J-Lat A1 was selected to have a silent HIV-1 LTR-driven provirus with the ability

173   to reactivate in response to TNFα (Jordan et al., 2003). The unique provirus within a

174   clone such as J-Lat A1 may be sensitive to position-dependent silencing effects (Chen

175   et al., 2016) and therefore may not accurately reflect the sensitivity of a population of

176   HIV-1 proviruses to transcriptional activation by Vpx or to silencing by FAM208A. To

177   address the effect of Vpx and FAM208A on on a population of proviruses with diverse

178   integration sites, Jurkat T cells were transduced with an HIV-1 LTR driven reporter

179   vector (LTR-*gfp)* that retains complete LTRs, *tat*, and *rev*, but has a frameshift mutation

180   in *env*, an *ngfr* reporter gene in place of *nef*, and *gfp* in place of *gag, pol, vif, and vpr*

181   (Fig. 3d). Four wks after transduction with LTR-GFP, the presence of latent proviruses

182   within the pool of Jurkat cells was confirmed by reactivation with either TNFα or TCR-

183   stimulation (Supplementary Fig. 3b). The Jurkat LTR-*gfp* cells were then transduced

184   with vectors expressing SIV$_{MAC}$251 Vpx or shRNA targeting FAM208A, and selected

185   with puromycin. Compared with control cells, *vpx* or FAM208A knockdown increased

186   the percentage of GFP$^+$ cells, whether cells were treated with TNFα or not (Figs 3e and

187   f). Similar results were obtained in three independently generated biological replicate

188   experiments, in which *vpx* was delivered or FAM208A was knocked down, from four to

189   eight wks after the first LTR-GFP transduction (Fig. 3f). Additionally, expression vectors

190   for SIV$_{MND2}$5440 Vpx, SIV$_{RCM}$02CM8081 Vpx, SIV$_{MND1}$GB1 Vpr, or SIV$_{AGM}$TAN1 Vpr all

191   increased GFP expression in Jurkat LTR-*gfp* cells (Supplementary Fig. 3c). Together,

192   these experiments demonstrate that FAM208A contributes to the transcriptional

193   repression of clonal or polyclonal LTR reporter lines, and that primate immunodeficiency

194   viruses counteract this activity via their Vpx and Vpr proteins.

195   The effect of Vpx or FAM208A knockdown on spreading infection with

196   replication-competent primate immunodeficiency viruses was tested next. Jurkat T cells

197   transduced to express SIV$_{MAC}$251 *vpx*, or cells transduced with control vector, were

198   infected with HIV-1-ZsGreen, a replication-competent HIV-1$_{NL4-3}$ clone, that encodes

199   ZsGreen in place of *nef* (Supplementary Table 1). Infection was monitored by

200   determining the percent ZsGreen$^+$ cells with flow cytometry, every two days for ten

201   days. Compared with the control, HIV-1 replication kinetics was accelerated by *vpx* (Fig.

202   4a). In similar fashion, HIV-1 infection of Jurkat cells transduced with the FAM208A

203   knockdown vector resulted in faster replication kinetics (Fig. 4b).

204   HIV-1 vpr has no detectable effect on HIV-1 replication in tissue culture

205   spreading infections with dividing target cells (Miller et al., 2017). This is presumably

206   related to the cell cycle arrest toxicity (Chang et al., 2004; Goh et al., 1998; He et al.,

207   1995; Re et al., 1995), and selection against *vpr* in tissue culture, since the effects of

208   *vpr* on HIV-1 are evident when proviral expression is restricted to single cycle infection

209   or cells are arrested with aphidicolin (Goh et al., 1998). Nonetheless, *vpr* offers a

210   selective advantage in vivo since cloned *vpr* mutant virus was repaired when virus was

211   injected into replication permissive chimps, or in an infected person (Goh et al., 1998).

212        $SIV_{MAC}239$ does not replicate in Jurkat cells so CEMx174 cells were used to test

213   the effect of FAM208A and *vpx* on replication of this virus. As in Jurkat cells, FAM208A

214   knockdown increased HIV-1 replication kinetics in CEMx174 cells (Fig. 4c). Then,

215   CEMx174 cells transduced with FAM208A or control knockdown vectors were

216   challenged with $SIV_{MAC}239$ or $SIV_{MAC}239$-Δ*vpx* and replication was assessed by

217   measuring reverse transcriptase activity in the supernatant. In the absence of *vpx*,

218   $SIV_{MAC}239$ replicated slower than the wild-type virus in control knockdown CEMx174

219   cells (Fig. 4d). This delay in $SIV_{MAC}239$-Δ*vpx* replication kinetics was not observed when

220   FAM208A was knocked down (Fig. 4d). Replication of HIV-2$_{GH}$Δ*vpx* was undetectable in

221   control knockdown CEMx174 cells (Fig. 4e). However, FAM208A knockdown rescued

222   the replication of HIV-2$_{GH}$Δ*vpx* to the level of wild-type HIV-2$_{GH}$ in control cells (Fig. 4e).

223   These experiments indicate that FAM208A inhibits primate immunodeficiency virus

224   replication and that Vpx antagonizes this restriction, resulting in expression - or

225   increased expression - from integrated proviruses, permitting virus spread.

226   The experiments reported here demonstrated that *vpx* and *vpr* activate

227   transcription from silenced proviruses and that this activity was mimicked by knockdown

228   of each of the HUSH complex components. These two observations were then shown to

229   be linked by the finding that Vpx associated with, and promoted degradation of HUSH

230   complex protein FAM208A, in a DCAF1- and proteasome-dependent manner. Latent

231   provirus activation and human FAM208A degradation were exhibited by a broader

232   range of primate immunodeficiency *vpx* and *vpr* orthologues than are capable of

233   degrading human SAMHD1, perhaps due to the greater conservation and essential

234   nature of FAM208A. Vpx and FAM208A disruption were important for transcriptional

235   activation of latent HIV-1 provirus pools and for the ability of HIV-1, HIV-2, and SIV_{MAC}

236   to effectively spread through cultured $CD4^+$ T cells. Further understanding of the

237   contributions of Vpx and Vpr and of the HUSH complex proteins, in concert with other

238   transcriptional silencing mechanisms targeting HIV-1, is hoped to inform ongoing efforts

239   to control or eliminate proviruses in HIV-1 infected patients.

240 **METHODS**

241

242 **Plasmids.** Sequences encoding 3xFLAG N-terminal-tagged Vpx and Vpr proteins were

243 ordered as codon-optimized, gBlocks Gene Fragments (Integrated DNA Technologies;

244 http://www.idtdna.com/) and cloned into either the pscALPS vector (Neagu et al., 2009)

245 for transduction, or into pcDNA3.1 for transfection. pAPM-D4 is a truncated derivative of

246 the pAPM lentivector (Pertel et al., 2011b) that expresses the puromycin

247 acetyltransferase and miR30-based shRNA from the SFFV promoter. Supplementary

248 Table 1 lists all plasmids used here, with corresponding addgene accession numbers,

249 target sites used in particular knockdown vectors, and accession numbers for all the

250 Vpx and Vpr orthologues tested here. All plasmid DNAs and sequences are available at

251 https://www.addgene.org/Jeremy_Luban/.

252

253 **Cell culture.** Cells were cultured at 37°C in 5% CO_2 humidified incubators and

254 monitored for mycoplasma contamination using the Mycoplasma Detection kit (Lonza

255 LT07-318). HEK293 cells (ATCC) were used for viral production and were maintained in

256 DMEM supplemented with 10% FBS, 20 mM L-glutamine (ThermoFisher), 25 mM

257 HEPES pH 7.2 (SigmaAldrich), 1 mM sodium pyruvate (ThermoFisher), and 1x MEM

258 non-essential amino acids (ThermoFisher). Jurkat and CEMx174 cells (ATCC) were

259 cultured in RPMI-1640 supplemented with 10% heat inactivated FBS, 20 mM L-

260 glutamine, 25 mM HEPES pH 7.2, 1 mM sodium pyruvate, 1x MEM non-essential amino

261 acids and Pen/Strep (ThermoFischer) (RPMI-FBS complete). J-Lat A1 cells (Jordan et

12

262   al., 2003) (NIH AIDS Reagent Program, catalogue #9852, donated by Eric Verdin) were

263   cultured in RPMI-FBS complete media.

264   Leukopaks were obtained from anonymous, healthy, blood bank donors (New

265   York   Biologics,   Southhampton,   NY).   As   per   NIH   guidelines

266   (http://grants.nih.gov/grants/policy/hs/faqs_aps_definitions.htm), experiments with these

267   cells were declared non-human subjects research by the University of Massachusetts

268   Medical School Institutional Review Board. PBMCs were isolated from leukopaks by

269   gradient centrifugation on Histopaque-1077 (Sigma-Aldrich). CD4$^+$ T cells were

270   enriched from PBMCs using anti-CD4 microbeads (Miltenyi) and were >95% CD4$^+$.

271   CD4$^+$ T cells were cultured in RPMI-FBS complete media in the presence of 50 U/mL

272   hIL-2 (NIH AIDS Reagent Program, catalogue #136).

273

274   **Vector production**. HEK293 cells were seeded at 75% confluency in 6-well plates and

275   transfected with 6.25 µL Transit LT1 lipid reagent (Mirus) in 250 µL Opti-MEM (Gibco)

276   with 2.25 µg total plasmid DNA. Full replicating virus was produced by transfection of

277   2.25µg of the indicated plasmid. Lenti-GFP reporters, LTR-GFP reporter, and shRNA

278   lentivectors were produced by transfection of the lentivector, psPAX2 *gagpol* expression

279   plasmid, and the pMD2.G VSV G expression plasmid, at a DNA ratio of 4:3:1. Vpx

280   containing SIV-VLPs were produced by transfection at a 7:1 plasmid ratio of SIV3+ to

281   pMD2.G, and ∆Vpx SIV VLPs were produced the same way using SIV3+ ∆Vpx plasmid.

282   12 hrs after transfection, media was changed to the specific media for the cells that

13

283   were to be transduced. Viral supernatant was harvested 2 days later, filtered through a

284   0.45 µm filter, and stored at 4°C.

285

286   **Reverse Transcriptase assay**. Virions in the transfection supernatant were quantified

287   by a PCR-based assay for reverse transcriptase activity (Pertel et al., 2011b). 5 µl

288   transfection supernatant were lysed in 5 µL 0.25% Triton X-100, 50 mM KCl, 100 mM

289   Tris-HCl pH 7.4, and 0.4 U/µl RNase inhibitor (RiboLock, ThermoFisher). Viral lysate

290   was then diluted 1:100 in a buffer of 5 mM $(NH_4)_2SO_4$, 20 mM KCl, and 20 mM Tris–HCl

291   pH 8.3. 10 µL was then added to a single-step, RT PCR assay with 35 nM MS2 RNA

292   (IDT) as template, 500 nM of each primer (5'-TCCTGCTCAACTTCCTGTCGAG-3' and

293   5'-CACAGGTCAAACCTCCTAGGAATG-3'), and hot-start Taq (Promega) in a buffer of

294   20 mM Tris-Cl pH 8.3, 5 mM $(NH_4)_2SO_4$, 20 mM KCl, 5 mM $MgCl_2$, 0.1 mg/ml BSA,

295   1/20,000 SYBR Green I (Invitrogen), and 200 µM dNTPs. The RT-PCR reaction was

296   carried out in a Biorad CFX96 cycler with the following parameters: 42°C 20 min, 95°C 2

297   min, and 40 cycles [95°C for 5 s, 60°C 5 s, 72°C for 15 s and acquisition at 80°C for 5

298   s]. 3 part vector transfections typically yielded 10^6 RT units/µL.

299

300   **Transductions.** For generating pools of shRNA knockdown Jurkat and CEMx174 lines,

301   cells were plated at 10^6 cells/mL in RPMI-FBS complete and transduced with 10^7 RT

302   units of viral vector per 10^6 cells, followed by selection with 1 µg/ml puromycin

303   (InvivoGen, cat# ant-pr-1). To generate stable *gag-gfp* expressing Jurkat cells, cells

304   were transduced as for shRNA KD above, followed by selection with 5 µg/mL blasticidin

305   (InvivoGen, cat# ant-bl-1) at day 3 after transduction.

306

307 CD4$^+$ T cells were stimulated in RPMI-FBS complete, with 50 U/ml IL-2 and 5 µg/mL

308 PHA-P (Sigma, cat# L-1668). After 3 days, T cells were washed and replated at 3 x 10^6

309 cells/mL in RPMI-FBS complete, with 50 U/ml IL-2. Cells were transduced with 10^8 RT

310 units of viral vector per 10^6 cells followed by selection in 2 µg/mL puromycin.. After

311 selection, cells were re-plated in RPMI-FBS complete with 50 U/ml IL-2 at 3 x 10^6

312 cells/mL in RPMI-FBS complete and transduced again with the indicated GFP vectors,

313 10^8 RT units of viral vector per 10^6 cells. Transduced T cells were analyzed 4-5 days

314 after the 2nd transduction.

315

316 **Lentiviral Infections.** 5 x 10^5 Jurkat or CEMx174 cells were incubated with 5 x 10^7 RT

317 units of HIV-1$_{NL4.3}$, HIV-2$_{GH}$, HIV-2$_{GH}\Delta vpx$, SIV$_{MAC}$239, or SIV$_{MAC}$239Δvpx virus stocks

318 produced in HEK-293 cells for 12 hrs in RPMI-FBS complete media, followed by a wash

319 in media and replated in 1 mL of media. Cells were split every 2-3 days and analyzed.

320 For monitoring of HIV-1 ZsGreen infection, when cells were split, aliquots were fixed in

321 BD Cytofix followed by analysis of GFP$^+$ cells by flow cytometry to determine infection

322 levels. For monitoring of SIV and HIV-2 infections, 50 µL aliquots of supernatant were

323 analyzed for RT activity using the above described RT assay.

324

325 **Re-activation assays.** LTR-driven GFP re-activation assays were performed with 10

326 ng/ml hTNFα (Invivogen, cat# rcyc-htnf), or with 1 µg/ml soluble α-CD3 and α-CD28

327 antibody. α-CD3 antibody (clone OKT3) and α-CD28 antibody (clone CD28.2) were

328 provided by Lisa Cavacini (MassBiologics, Mattapan, Massachusetts).

329

330   **qRT-PCR.** Total RNA was isolated from Jurkat cells using Trizol reagent followed by

331   purification of RNA with RNeasy Plus Mini (Qiagen) with Turbo DNase (ThermoFisher)

332   in order to limit DNA contamination. First-strand synthesis used Superscript III Vilo

333   Master mix (Invitrogen) with random hexamers. qPCR was performed in 20 µL using

334   SYBR green reagent (Applied Biosystems) with primers designed against *gag, gfp,* and

335   *gapdh* for normalization. . Amplification was on a CFX96 Real Time Thermal Cycler

336   (Bio-Rad) using the following program: 95°C for 10 min, then 45 cycles of 95°C for 15 s

337   and 60°C for 60 s. Cells not transduced with Lenti-GFP vector were used as negative

338   control and the housekeeping gene GAPDH was used to normalize expression levels.

339   The primer sequences used were: *gag* primers *(*Forward: 5'-

340   GCTGGAAATGTGGAAAGGAA-3'; Reverse: 5'-AGTCTCTTCGCCAAACCTGA-3'), *gfp*

341   primers *(*Forward: 5'-GCAGAGGTGAAGTTCGAAGG-3'; Reverse: 5'-

342   CCAATTGGTGTGTTCTGCTG-3'), *gapdh* primers *(*Forward: 5'-

343   AGGGCTGCTTTTAACTCTGGT-3'; Reverse: 5'-CCCCACTTGATTTTGGAGGGA-3').

344

345   **Flow cytometry.** Cells were fixed in BD Cytofix Buffer prior to data acquisition on a BD

346   C6 Accuri. Data was analyzed in FlowJo.

347

348   **Western Blot.** Cells were washed in PBS, counted, normalized for cell number, and

349   lysed directly in 1x SDS-PAGE sample buffer. Samples were run on NuPage 4-12%

350   Bis-Tris gels followed by blotting onto nitrocellulose membranes. Primary antibodies

351   used: FAM208A (Atlas, HPA00875), MPHOSPH8 (Proteintech, 16796-1-AP), PPHLN1

352 (Sigma, HPA038902), SETDB1 (Proteintech 11231-1-AP), DCAF1 (Proteintech, 11612-

353 1-AP), FLAG (Novus, NB600-345), FLAG (Sigma, F1804, used for IP), and HA

354 (Biolegend, 901501).

355

356 **Vpr and Vpx phylogeny.** The following Vpr and Vpx amino acid sequence alignments

357 were obtained from the Los Alamos National Laboratories (LANL) HIV sequence

358 database: 2016 HIV-1/SIVcpz Vpr, 2016 HIV-2/SIVsmm Vpr, 2016 HIV-2/SIVsmm Vpx,

359 2016 other SIV Vpr, and 2016 other Vpx. Consensus sequences were generated for

360 HIV-1 group M subtypes A, B, C, D, F, G, H, I, J, and those designated U in the LANL

361 database, as well as group N. A master alignment was scaffolded from the above

362 alignments and re-aligned by hand. Redundant SIV and HIV-2 Vpr and Vpx sequences

363 were removed, and the sequences of individual HIV-1 isolates were replaced with the

364 consensus sequences. This was used to generate a master phylogeny using RAxML

365 8.2.11, as implemented in Geneious with gamma LG substitution model and Rapid

366 Bootstrapping with search for best scoring tree algorithm. This master tree was utilized

367 to identify major relationships and identify a reduced number of sequences to retain

368 while maintaining the overall phylogenic structure. Vpx and Vpr sequences from the

369 following viral isolates were retained: HQ179987, L20571, M15390, AF208027,

370 AB731738, KP890355, M15390, AF208027, AB731738, KP890355, U58991, M30931,

371 L40990, KJ461715, AF301156, U42720, AY169968, DQ373065, DQ373064,

372 DQ374658, FJ919724, AJ580407, KM378563, KM378563, FJ424871, M66437,

373 AF468659, AF468658, AF188116, M76764, LC114462, M27470, AY159322,

374 AY159322, U79412, U79412, AY340701, AY340700, EF070329, KF304707,

375   FM165200, HM803690, HM803689, AF382829, AF349680, HM803690, HM803689,

376   AF349680, U04005, JX860432, JX860430, JX860426, JX860432, M83293, M83293,

377   AF131870, AY523867, AM182197, AM713177, U26942, and the HIV-1 group M clade B

378   consensus. These sequences were used to generate a phylogeny using the same

379   method as above. Superfluous taxa were pruned from this phylogeny using Mesquite

380   3.4 and the resulting tree was visualized in FigTree v1.4.3.

381

382   **Sampling**. At least three biological replicates were performed for all experiments. The

383   screen for factors mediating silencing of the Lenti-GFP vector utilized 3 target

384   sequences for each candidate gene. Flow cytometry plots in the figures show

385   representative data taken from experiments performed at the same time. HIV-1, HIV-2,

386   and SIV spreading experiments were repeated 3 times each and representative data of

387   one such experiment is shown.

388

389   **Statistics.** Information regarding the statistical tests utilized, and the n values, are

390   found in the figure legends. Statistical analysis of the knockdown screen of factors

391   involved in silencing of Lenti-GFP was analyzed by one-way ANOVA with Dunnett post

392   test comparing 3 shRNA target sites to control knockdown conditions. All statistics

393   presented were performed using PRISM 5.0 (GraphPAD Software, La Jolla, CA).

REFERENCES

Baldauf, H.-M., Pan, X., Erikson, E., Schmidt, S., Daddacha, W., Burggraf, M., Schenkova, K., Ambiel, I., Wabnitz, G., Gramberg, T., et al. (2012). SAMHD1 restricts HIV-1 infection in resting CD4(+) T cells. Nat. Med. *18*, 1682–1687.

Chang, F., Re, F., Sebastian, S., Sazer, S., and Luban, J. (2004). HIV-1 Vpr induces defects in mitosis, cytokinesis, nuclear structure, and centrosomes. Mol. Biol. Cell *15*, 1793–1801.

Chen, H.-C., Martinez, J.P., Zorita, E., Meyerhans, A., and Filion, G.J. (2016). Position effects influence HIV latency reversal. Nat. Struct. Mol. Biol. *24*, nsmb.3328.

Chéné, I. du, Basyuk, E., Lin, Y.-L., Triboulet, R., Knezevich, A., Chable-Bessia, C., Mettling, C., Baillat, V., Reynes, J., Corbeau, P., et al. (2007). Suv39H1 and HP1γ are responsible for chromatin-mediated HIV-1 transcriptional silencing and post-integration latency. EMBO J. *26*, 424–435.

Fregoso, O.I., Ahn, J., Wang, C., Mehrens, J., Skowronski, J., and Emerman, M. (2013). Evolutionary toggling of Vpx/Vpr specificity results in divergent recognition of the restriction factor SAMHD1. PLoS Pathog. *9*, e1003496.

Goh, W.C., Rogel, M.E., Kinsey, C.M., Michael, S.F., Fultz, P.N., Nowak, M.A., Hahn, B.H., and Emerman, M. (1998). HIV-1 Vpr increases viral expression by manipulation of the cell cycle: a mechanism for selection of Vpr in vivo. Nat. Med. *4*, 65–71.

Goujon, C., Jarrosson-Wuillème, L., Bernaud, J., Rigal, D., Darlix, J.-L., and Cimarelli, A. (2006). With a little help from a friend: increasing HIV transduction of monocyte-derived dendritic cells with virion-like particles of SIV(MAC). Gene Ther. *13*, 991–994.

He, J., Choe, S., Walker, R., Di Marzio, P., Morgan, D.O., and Landau, N.R. (1995). Human immunodeficiency virus type 1 viral protein R (Vpr) arrests cells in the G2 phase of the cell cycle by inhibiting p34cdc2 activity. J. Virol. *69*, 6705–6711.

Hrecka, K., Hao, C., Gierszewska, M., Swanson, S.K., Kesik-Brodacka, M., Srivastava, S., Florens, L., Washburn, M.P., and Skowronski, J. (2011). Vpx relieves inhibition of HIV-1 infection of macrophages mediated by the SAMHD1 protein. Nature *474*, 658–661.

Jordan, A., Bisgrove, D., and Verdin, E. (2003). HIV reproducibly establishes a latent infection after acute infection of T cells in vitro. EMBO J. *22*, 1868–1877.

Laguette, N., Sobhian, B., Casartelli, N., Ringeard, M., Chable-Bessia, C., Ségéral, E., Yatim, A., Emiliani, S., Schwartz, O., and Benkirane, M. (2011). SAMHD1 is the dendritic- and myeloid-cell-specific HIV-1 restriction factor counteracted by Vpx. Nature *474*, 654–657.

429 Lim, E.S., Fregoso, O.I., McCoy, C.O., Matsen, F.A., Malik, H.S., and Emerman, M.
430 (2012). The ability of primate lentiviruses to degrade the monocyte restriction factor
431 SAMHD1 preceded the birth of the viral accessory protein Vpx. Cell Host Microbe *11*,
432 194–204.

433 McCarthy, K.R., and Johnson, W.E. (2014). Plastic proteins and monkey blocks: how
434 lentiviruses evolved to replicate in the presence of primate restriction factors. PLoS
435 Pathog. *10*, e1004017.

436 Miller, C.M., Akiyama, H., Agosto, L.M., Emery, A., Ettinger, C.R., Swanstrom, R.I.,
437 Henderson, A.J., and Gummuluru, S. (2017). Virion-Associated Vpr Alleviates a
438 Postintegration Block to HIV-1 Infection of Dendritic Cells. J. Virol. *91*.

439 Neagu, M.R., Ziegler, P., Pertel, T., Strambio-De-Castillia, C., Grütter, C., Martinetti, G.,
440 Mazzucchelli, L., Grütter, M., Manz, M.G., and Luban, J. (2009). Potent inhibition of
441 HIV-1 by TRIM5-cyclophilin fusion proteins engineered from human components. J.
442 Clin. Invest. *119*, 3035–3047.

443 Pertel, T., Reinhard, C., and Luban, J. (2011a). Vpx rescues HIV-1 transduction of
444 dendritic cells from the antiviral state established by type 1 interferon. Retrovirology *8*,
445 49.

446 Pertel, T., Hausmann, S., Morger, D., Züger, S., Guerra, J., Lascano, J., Reinhard, C.,
447 Santoni, F.A., Uchil, P.D., Chatel, L., et al. (2011b). TRIM5 is an innate immune sensor
448 for the retrovirus capsid lattice. Nature *472*, 361–365.

449 Peterlin, B.M., Liu, P., Wang, X., Cary, D., Shao, W., Leoz, M., Hong, T., Pan, T., and
450 Fujinaga, K. (2017). Hili Inhibits HIV Replication in Activated T Cells. J. Virol. *91*.

451 Re, F., Braaten, D., Franke, E.K., and Luban, J. (1995). Human immunodeficiency virus
452 type 1 Vpr arrests the cell cycle in G2 by inhibiting the activation of p34cdc2-cyclin B. J.
453 Virol. *69*, 6859–6864.

454 Reinhard, C., Bottinelli, D., Kim, B., and Luban, J. (2014). Vpx rescue of HIV-1 from the
455 antiviral state in mature dendritic cells is independent of the intracellular
456 deoxynucleotide concentration. Retrovirology *11*, 12.

457 Sharova, N., Wu, Y., Zhu, X., Stranska, R., Kaushik, R., Sharkey, M., and Stevenson,
458 M. (2008). Primate lentiviral Vpx commandeers DDB1 to counteract a macrophage
459 restriction. PLoS Pathog. *4*, e1000057.

460 Srivastava, S., Swanson, S.K., Manel, N., Florens, L., Washburn, M.P., and
461 Skowronski, J. (2008). Lentiviral Vpx accessory factor targets VprBP/DCAF1 substrate
462 adaptor for cullin 4 E3 ubiquitin ligase to enable macrophage infection. PLoS Pathog. *4*,
463 e1000059.

464 Tchasovnikarova, I.A., Timms, R.T., Matheson, N.J., Wals, K., Antrobus, R., Göttgens,
465 B., Dougan, G., Dawson, M.A., and Lehner, P.J. (2015). GENE SILENCING. Epigenetic

466 silencing by the HUSH complex mediates position-effect variegation in human cells.
467 Science *348*, 1481–1485.

468 Tchasovnikarova, I.A., Timms, R.T., Douse, C.H., Roberts, R.C., Dougan, G., Kingston,
469 R.E., Modis, Y., and Lehner, P.J. (2017). Hyperactivation of HUSH complex function by
470 Charcot-Marie-Tooth disease mutation in MORC2. Nat. Genet.

471 Wang, G.Z., and Goff, S.P. (2017). Transcriptional Silencing of Moloney Murine
472 Leukemia Virus in Human Embryonic Carcinoma Cells. J. Virol. *91*.

473 Weinberg, M.S., and Morris, K.V. (2016). Transcriptional gene silencing in humans.
474 Nucleic Acids Res. *44*, 6505–6517.

475 Wolf, D., and Goff, S.P. (2007). TRIM28 mediates primer binding site-targeted silencing
476 of murine leukemia virus in embryonic cells. Cell *131*, 46–57.

ACKNOWLEDGEMENTS

Author Contributions: L.Y. and J.L. designed the experiments. L.Y. performed the experiments with assistance from M.H.G., K.K., S.L.G., S.M., A.D., and W.E.D., L.Y. and J.L. analyzed the experimental data. All authors contributed to the writing of the manuscript.

Competing interests: None declared.

Data and materials availability: all data needed to evaluate the conclusions in the paper are present in the paper or in the supplementary table. The plasmids described in Supplementary Table 1, along with their complete nucleotide sequences, are available at https://www.addgene.org/Jeremy_Luban/. Correspondence and requests for materials should be addressed to J.L. (jeremy.luban@umassmed.edu).

498 **Figure Legends**

499

500 **Figure 1. Diverse primate immunodeficiency virus *vpx* and *vpr* orthologues activate**

501 **provirus transcription, whether delivered before, during, or after reporter provirus**

502 **integration.**

503 **a,** Schematic of experimental protocol in (**b**). **b,** Flow cytometry plot showing percent GFP$^+$

504 Jurkat cells after sequential transduction with the indicated lentivectors, followed by exposure to

505 the indicated VLPs. **c,d,** Histogram of flow cytometry signal in Jurkat cells transduced with *gfp-*

506 reporter virus, and either exposed to the indicated VLPs (**c**), or transduced with the indicated

507 vectors (**d**). **e,** Phylogenetic tree showing evolutionary relationship of Vpx and Vpr proteins. The

508 transactivation activity of Jurkat reporter lines, tested as in (**d**), and human SAMHD1

509 degradation activity (Lim et al., 2012), are indicated. $\varnothing$ indicates Vprs that were too toxic (G2

510 arrest) for assessment. All data shown is representative of at least three biological replicates.

511

512 **Figure 2. Vpx activates provirus transcription by degrading HUSH complex components**

513 **a,** Jurkat cells transduced with shRNA-puro^R vectors targeting the indicated genes were

514 selected with puromycin, transduced with Lenti 2-Δ*vpx*, and analyzed 5 days later. Plot depicts

515 GFP signal in knockdown lines relative to Jurkats bearing SIV$_{MAC}$251 *vpx* (mean ± S.E.M., n=3

516 shRNA target sites). *, *P*<0.05 as determined by 1-way ANOVA with Dunnett post-test, relative

517 to luciferase knockdown control. **b,** Jurkat cells were transduced with the indicated shRNA-

518 puro^R vectors and selected with puromycin. Resistant cells were transduced with *vpx$^+$* or Δ*vpx*

519 Lenti 2 vector, and analyzed for GFP expression 7 days later. **c,** Immunoblot analysis for

520 components of the HUSH complex in Jurkat cells expressing shRNA constructs used in (**b**). **d,**

521 CD4$^+$ T cells were activated for 3 days with PHA and then transduced and assayed as in (**b**). **e,**

522 Immunoblot analysis of Jurkat lines transduced to express *vpx* from SIV$_{MAC}$251, SIV$_{RCM}$NG411,

523   SIV$_{MND2}$5440, or control. **f,** Levels of HUSH components in (**e**) shown as shRNA treated

524   condition relative to control. **g,** FAM208A, DCAF1, and Actin immunoblot of Jurkat cells

525   transduced with DCAF1 shRNA-puro^R vector or control, that were treated with Vpx$^+$ or ΔVpx

526   VLPs for 18 hrs. **h,** HEK293 cells were co-transfected with HA-FAM208A and the indicated

527   FLAG-Vpx constructs. 18 hrs after transfection, cells were either exposed to proteasome

528   inhibitor PR171 or left untreated. 8 hrs after inhibitor treatment cells were lysed, FLAG-Vpx was

529   immunoprecipitated, and immunoblotted for FLAG-Vpx and HA-FAM208A. Immunoblotting of
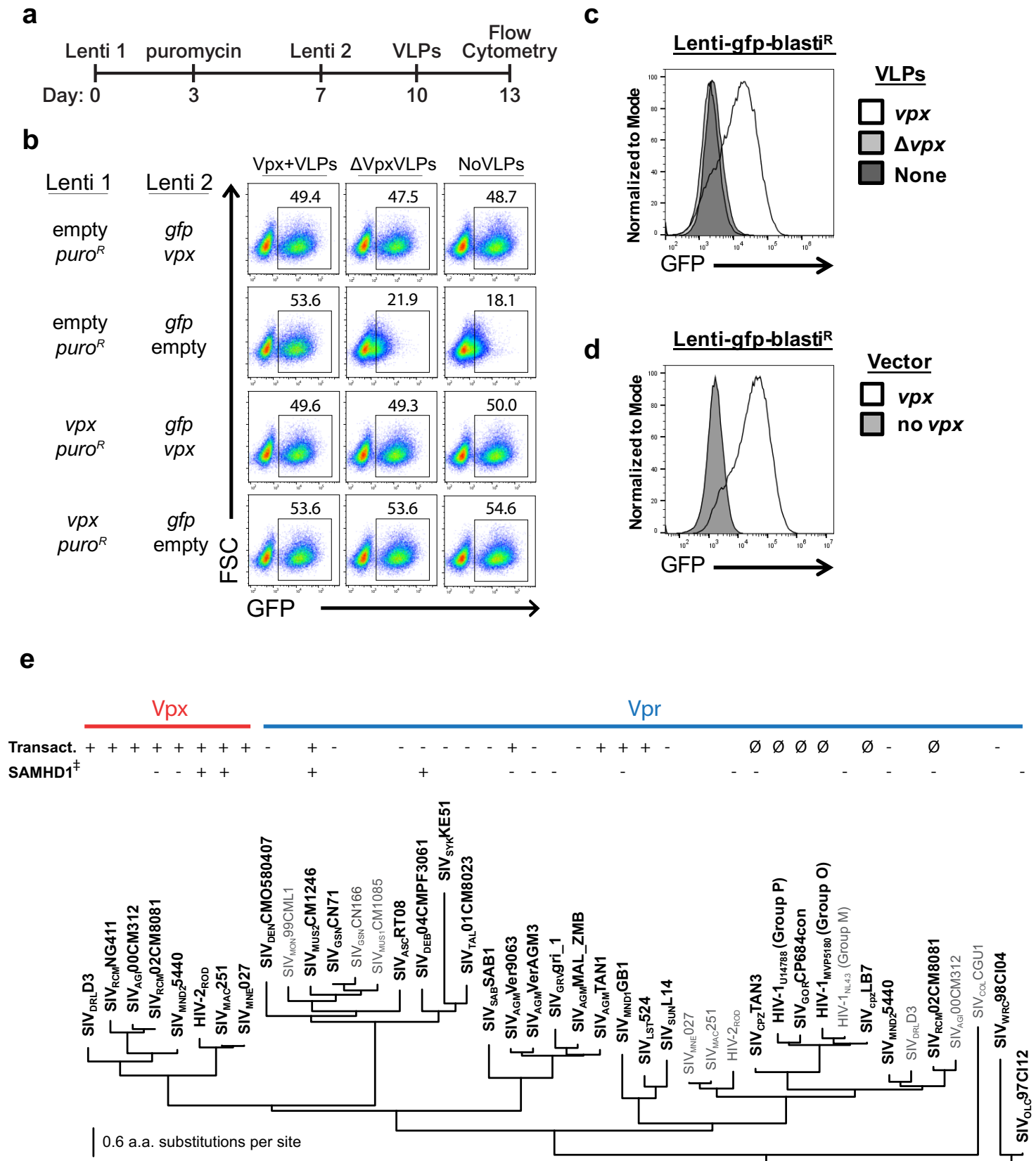
530   input lysates are shown below.

531

532   **Figure 3. The HIV-1 LTR is activated by Vpx or disruption of FAM208A**
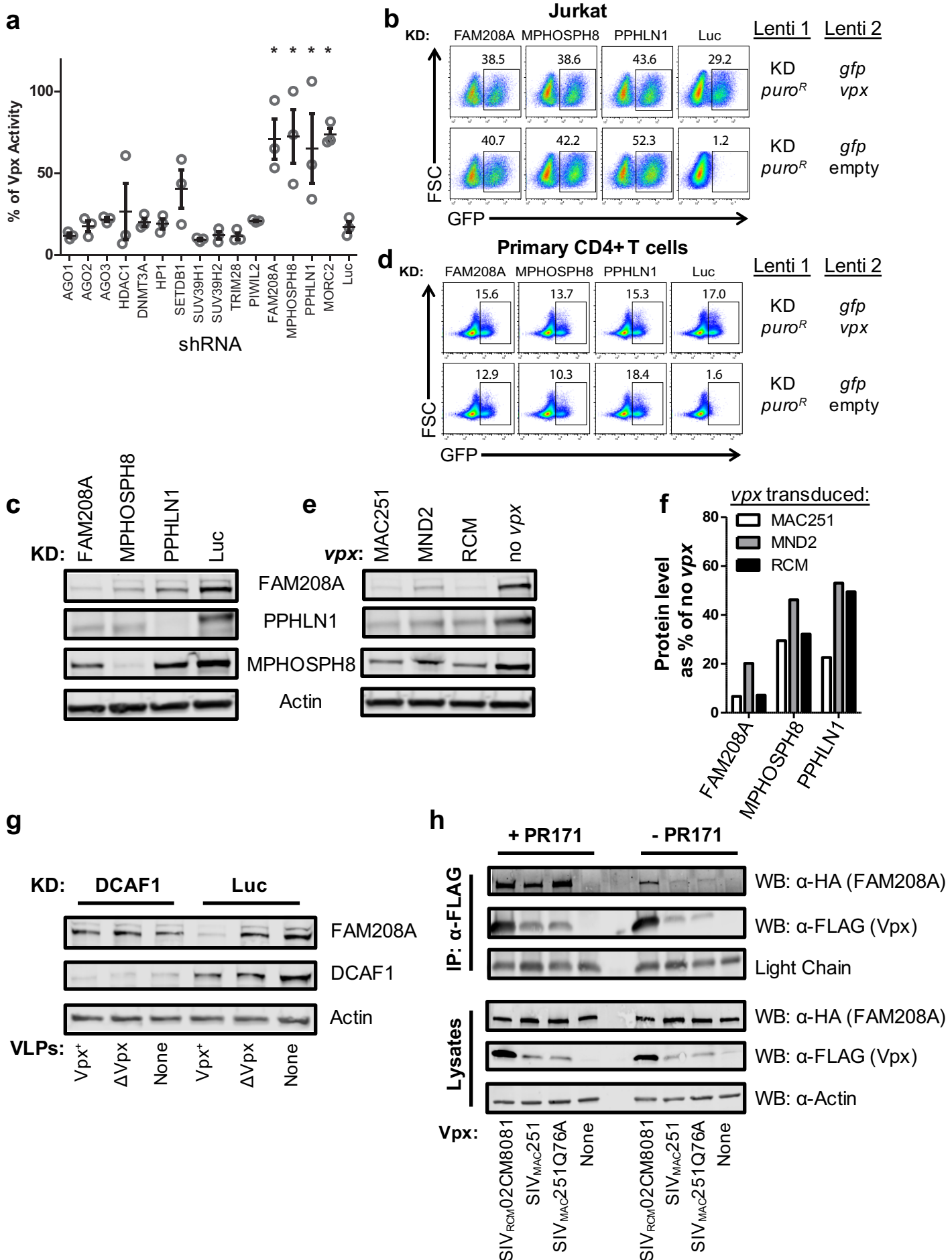
533   **a,** Schematic of the HIV-1 minigenome integrated in the J-Lat A1 line. **b,** J-Lat A1 cells were

534   transduced with Lenti 1 encoding SIV$_{MAC}$251 *vpx* or Δ*vpx* control, or with lentivectors expressing

535   shRNA targeting FAM208A or luciferase control. Transduced cells were selected with

536   puromycin, and activated for 24 hrs with 10 ng/ml of TNFα. Representative GFP signal by flow

537   is shown. **c,** Quantification of results from (**b**) and additional replicates (mean ± S.E.M., n=3

538   independent experiments). *, *P<0.02* **d,** Schematic of the LTR-*gfp* provirus used to analyze HIV-

539   1 LTR driven *gfp* expression in pools of cells. **e,** Jurkat cells transduced with LTR-*gfp* were kept

540   in culture for 4 wks and then transduced and assessed by flow cytometry, as in (**b**). **f,**

541   Quantification of results from (**e**) (mean ± S.E.M., n=4 independent experiments) *, *P<0.02*

542

543   **Figure 4. Vpx counteracts FAM208A restriction of HIV-1, SIV$_{MAC}$239, or HIV-2$_{GH}$, during**

544   **spreading infection in CD4$^+$ T cells.**

545   **a,b,** Replication of HIV-1-ZsGreen in Jurkat cells transduced with SIV$_{MAC}$251 *vpx* or

546   control (**a**), or with lentivectors expressing shRNA targeting FAM208A or Luc control (**b**).

547 Replication kinetics was measured by flow cytometry for ZsGreen$^+$ cells. **c,d,e,**

548 Spreading infection of HIV-1-ZsGreen (**c**), SIV$_{MAC}$239 or SIV$_{MAC}$239Δvpx (**d**), and HIV-

549 2$_{GH}$ or HIV-2$_{GH}$ Δvpx virus in CEMx174 cells transduced with FAM208A or Luc control

550 shRNA. Spread of HIV-1-ZsGreen was assessed by flow cytometry as in (**a**), while

551 spread of SIV$_{mac}$239 (**b**) and HIV-2$_{GH}$ (**c**) was assessed by measuring the accumulation

552 of reverse transcriptase (RT) activity in the supernatant. All data is representative of
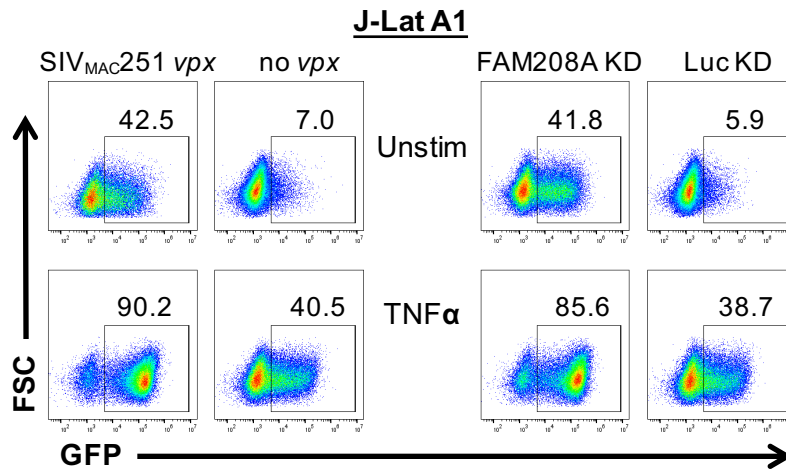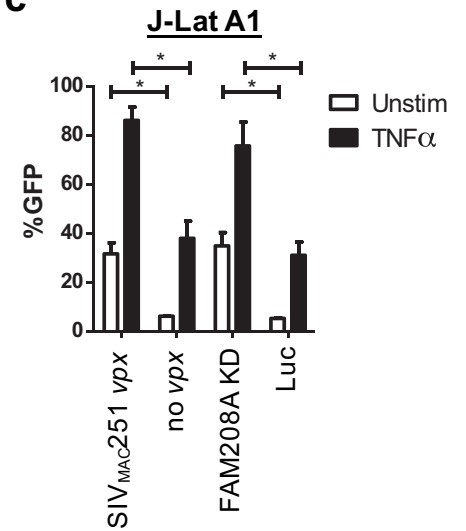
553 three repeat experiments.

Yurkovetskiy et al, Fig. 1

Yurkovetskiy et al, Fig. 2

a Provirus in J-Lat A1

| 5' LTR | *tat* | IRES | *gfp* | 3' LTR |

b J-Lat A1

SIV$_{MAC}$251 *vpx* | no *vpx* | FAM208A KD | Luc KD

42.5 | 7.0 | 41.8 | 5.9 — Unstim

90.2 | 40.5 | 85.6 | 38.7 — TNFα

FSC / GFP

c J-Lat A1

%GFP

☐ Unstim ■ TNFα

SIV$_{MAC}$251 *vpx* | no *vpx* | FAM208A KD | Luc

d LTR-*gfp*

5' LTR | *gfp* | *vpu* | *tat* | *env* | *f/s* | *rev* | *ngfr* | 3' LTR

e Jurkat – LTR-*gfp*

SIV$_{MAC}$251 *vpx* | no *vpx* | FAM208A KD | Luc KD

14.8 | 2.7 | 26.7 | 1.1 — Unstim

51.2 | 14.0 | 51.6 | 4.1 — TNFα

FSC / GFP

f Jurkat – LTR-*gfp*

%GFP

☐ Unstim ■ TNFα

SIV$_{MAC}$251 *vpx* | no *vpx* | FAM208A KD | Luc

Yurkovetskiy et al, Fig. 3

a HIV-1 in Jurkat

vpx

no *vpx*

b HIV-1 in Jurkat

FAM208A KD

Luc KD

c HIV-1 in CEMx174

FAM208A KD

Luc KD

d SIV$_{MAC}$239 in CEMx174

FAM208A KD/
SIV$_{MAC}$239Δ*vpx*

Luc KD/
SIV$_{MAC}$239Δ*vpx*

Luc KD/SIV$_{MAC}$239

e HIV-2$_{GH}$ in CEMx174

FAM208A KD/
HIV-2$_{GH}$Δ*vpx*

Luc KD/
HIV-2$_{GH}$Δ*vpx*

Luc KD/HIV-2$_{GH}$

Yurkovetskiy et al, Fig. 4